Fine structure of the developing epidermis in the embryo of the American alligator (*Alligator mississippiensis*, Crocodilia, Reptilia)

LORENZO ALIBARDI[1] AND MICHAEL B. THOMPSON[2]

[1]*Dipartimento di Biologia, University of Bologna, Bologna, Italy, and* [2]*School of Biological Sciences and Wildlife Institute, University of Sydney, NSW 20006, Sydney, Australia*

(*Accepted 6 September 2000*)

ABSTRACT

The morphological transition from the simple epidermis that contacts the amniotic fluid of embryonic crocodilians to the adult epidermis required in a terrestrial environment has never been described. We used light and electron microscopy to study the development, differentiation and keratinisation of the epidermis of the American alligator, *Alligator mississippiensis*, between early and late stages of embryonic skin formation. In early embryonic development, the epidermis consists of a flat bilayer. As it develops, the bilayered epidermis comes to lie beneath the peridermis. Glycogen is almost absent from the bilayered epidermis but increases in basal and suprabasal cells when scales form. Glycogen disappears from suprabasal cells that accumulate keratin. The peridermis and 1 or 2 subperidermal layers form an embryonic epidermis that is partially or totally lost before hatching. These cells accumulate coarse filaments and form reticulate bodies. Mucous and lamellate granules are produced in the Golgi apparatus and are partly secreted extracellularly. The embryonic cells darken with the formation of larger reticulate bodies that aggregate with intermediate filaments and other cell organelles, as their nuclear chromatin condenses. Thin β-cells resembling those of scutate scales of birds develop beneath the embryonic epidermis and form a stratified β-layer that varies in thickness in different body regions. The epidermis differentiates first in the back, tail and belly. At the beginning of β-cell differentiation, the cytoplasm contains sparse bundles of α-keratin filaments, glycogen and lipid droplets or vacuoles apparently derived from the endoplasmic reticulum and Golgi apparatus. These organelles disappear rapidly as irregular bundles of electron-dense β-keratin filaments accumulate and form larger bundles. The larger bundles consist of 3 nm thick electron-pale keratin microfibrils and are derived from the assemblage of β-keratin molecules produced by ribosomes. While in mammals the epidermal barrier is formed by α-keratinocytes, in the alligator the barrier is formed by β-keratin cells. The β-layer is reduced or absent from the small hinge region between scales. In the latter areas the barrier is made of α or a mixture of α/β keratinocytes. Thus alligators resemble birds where the β-keratin molecules are deposited directly over an α-keratin scaffold, rather than an initial production of β-keratin packets which then merge with α-keratin, as occurs in the Chelonia and Lepidosauria. The pigmentation of the epidermis of embryos is mostly derived from epidermal melanocytes.

Key words: Alligator; embryos; epidermis; keratinisation; ultrastructure.

INTRODUCTION

Reptiles typically have scaly skin, but the shape, dimension, histological and fine structure of scales vary in different areas of the body, suggesting functional differences (Alexander, 1970; Roth & Jones, 1970; Maderson, 1985; Landmann, 1986; Irish et al. 1988; Maderson et al. 1998). Among reptiles, the crocodilians show extreme variation of scale shapes (Brazaitis, 1987), although all scales consist of scutes with little overlap or are plate-like, and are characterised by an expanded outer surface, a short inner surface and a hinge region (Lange, 1931; Lillywhite & Maderson, 1982; Landmann, 1986).

Correspondence to Dr L. Alibardi, Dipartimento di Biologia, via Selmi 3, 40126, Bologna, Italy. Tel.: +39 51 209 4249; fax: +39 51 251208.

The dorsal and ventral scales of crocodilians contain β-keratin on the outer surface (Spearman, 1966; Baden & Maderson, 1970), while α-keratin (or a mix of α- and β-keratin) is limited to the hinge region (Alexander, 1970; Parakkal & Alexander, 1972). It is not known, however, whether the other body scales follow the same pattern of keratinisation as the dorsal and ventral scales. The tough β-keratin differs from α-keratin in having a lower molecular weight (14–25 kDa vs 40–70 kDa for α-keratin), an amino acid composition rich in repetitive sequences containing glycine and proline, a secondary structure of β-pleated sheets, a molecular organisation of keratin molecules of different microfibrillar diameter and ultrastructural pattern (2–3 nm vs 8–12 nm for α-keratin), and a higher resistance to distension than α-keratin (Baden & Maderson, 1970; Wyld & Brush, 1979, 1983; Carver & Sawyer, 1987, 1988, 1989; Shames et al. 1988; Sawyer et al. 2000). Furthermore, at the beginning of differentiation, α-keratin cells contain many bundles of intermediate filaments together with lipid among the lamellar bodies and have little matrix material (few sulphide and disulphide bonds). In contrast, β-keratin cells contain few bundles of intermediate filaments and little lipid, but an extensive matrix with many disulphide bonds (Spearman, 1966; Parakkal & Alexander, 1972; Baden et al. 1974; Landmann, 1986).

The process of β-keratinisation in crocodilians has not been described in detail and the only available data concern keratinised cells of the adult epidermis (Alexander, 1970; Parakkal & Alexander, 1972). The initial production of β-keratin, its packing into larger keratin bundles and the formation of the β-keratin pattern (Baden & Maderson, 1970) remain to be studied, especially in the embryo. The pattern of scalation, keratinisation and pigmentation are established during embryogenesis (Ferguson, 1985, 1987), but the details of development are undescribed.

In this study, we have extended our survey of the process of keratinisation in the developing epidermis of extant reptiles to the American alligator, *Alligator mississippiensis*, as a representative of crocodilians. In so doing, we aim to compare crocodiles with other reptiles for which there are data, the lepidosaurs (Alibardi, 1998*a*, *b*, 1999; Alibardi & Thompson, 1999*a*) and turtles (Alibardi & Thompson, 1999*b*, *c*), and, as the nearest living relative of ancestral archosaurs, compare our results with the process of keratinisation in birds (Parakkal & Alexander, 1972; Spearman & Hardy, 1985; Maderson & Alibardi, 2000; Alibardi, 2000).

MATERIALS AND METHODS

Eggs from 3 clutches of *Alligator mississippiensis* were obtained from the Australian Reptilian Park at Gosford, NSW. Eggs were incubated half buried in moistened vermiculite with a water potential of -150 kPa in boxes at 29–30 °C. Embryos were removed from eggs and fixed for microscopy throughout incubation. The following embryonic stages (ES), based on Ferguson (1985, 1987), were studied: ES13 (n = 2), ES16 (n = 2), ES18 (n = 2), ES19 (n = 2), ES20 (n = 2), ES21 (n = 3), ES22 (n = 3), ES23 (n = 4), ES24 (n = 5), ES25 (n = 1).

Some embryos were fixed whole in 10% formaldehyde for 24–48 h and preserved in 80% ethanol for light microscopy. Other embryos were decapitated; small specimens were dissected into pieces 1–3 mm in length, whereas larger embryos (from ES21 onwards) had pieces of skin (1–4 mm × 1–3 mm) dissected from 7 different areas of the body (Brazaitis, 1987): neck, gular, dorsal, limbs (including digits), flank, ventral (belly), tail. Some of the tissues were fixed for 6–9 h in cold (4 °C) 2.5% glutaraldehyde in 0.1 M phosphate buffer at pH 7.2–7.4. After 30 min rinsing in the same buffer, the tissues were placed for 90–120 min in 2% OsO_4, rinsed, dehydrated in ethanol, immersed in 2 changes of propylene oxide (15–20 min each) and embedded in Spurr's resin. Some tissues were fixed in 10% buffered formaldehyde for 12–24 h, dehydrated in ethanol, cleared in xylene and embedded in wax. Other tissues were fixed in Carnoy's fluid for 9–12 h, dehydrated in 80% ethanol, and embedded in hydrophilic resins (JB-4 or Bioacryl).

Semithin sections (1–2 μm) were cut with an ultramicrotome, stained with 1% toluidine blue, and observed for orientation using a light microscope. Some of these sections were stained with periodic acid Schiff (PAS) to detect glycogen and compared with sections after α-amylase digestion (as a control for glycogen localisation) (Mazzi, 1977).

Thin sections (50–90 nm) of skin from all body regions were cut with an ultramicrotome and collected on copper or nickel grids. After routine contrasting with uranyl acetate and lead citrate, the grids were observed with a Philips CM 100 electron microscope operating at 60–80 kV.

RESULTS

Gross observations

The skin of the embryo at ES13–16 is smooth and unpigmented (Fig. 1*A*). Undulations in the epidermis

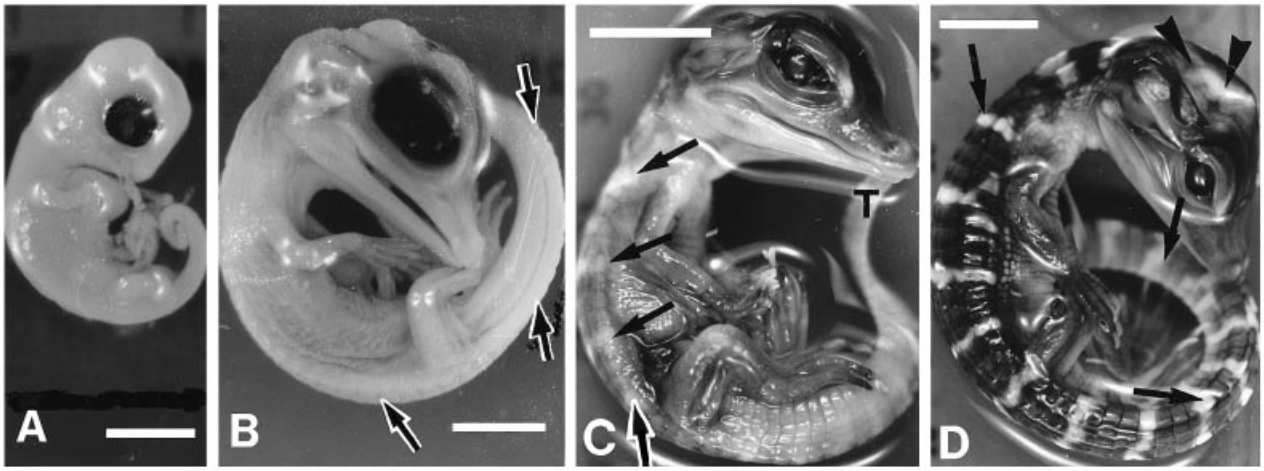

Fig. 1. Four representative embryonic stages (ES) of the American alligator, *Alligator mississippiensis*. (*A*), embryo at ES16 showing the unpigmented smooth skin and limbs at the palette stage (digits not yet formed) of development. Bar, 5 mm. (*B*), embryo at ES21 showing the lengthening snout, some diffuse but very faint pigmentation and scalation on the tail and back (arrows). Bar, 5 mm. (*C*), embryo at ES23 with the beginning of banding (arrows), diffuse scalation and well developed claws. T, tail. Bar, 10 mm. (*D*), embryo at ES24 showing heavy pigmentation, scales and distinct bands (arrows), but with brain case still open (arrowheads). Bar, 10 mm.

outline initial scale formation on the tail and lower back at ES18. The embryo shows the first weak pigmentation in the dorsal tail, ear area, arms and thighs at ES21 (Fig. 1*B*). Recognisable scalation is present, essentially on the tail and middle of the back where the first scales are formed. At ES21–22, the pigmentation becomes more extensive although still weak, particularly on the forehead, jaw and back, while scale anlagen are present on the back, tail (both dorsal and ventral), belly and some proximal areas of limbs where few scales are visible. Scales are less differentiated or still absent in the gular, head, jaw, flank, distal limbs, and digit areas. The braincase is open, showing large portions of the developing brain. At ES23, scales have developed over most body areas (Fig. 1*C*) but are still absent or poorly developed over the jaws, head, distal limbs and digits. The skin is still soft and easily cut or damaged at this stage. Although the body pigmentation is still faint, the first dorsolateral pigmented bands are visible. At this stage, fingers and toes are completely separate and claws are forming. The braincase opening is smaller but large brain areas are still visible. At ES24, the embryo is almost completely pigmented and the characteristic dorsoventral pale bands are obvious and reach the belly and ventral side of the tail (Fig. 1*D*). On the toes claws are well developed but blunt. The braincase opening is reduced but still present. Scales are present all over the body surface and are more pigmented than in the previous stage. The skin is tougher to cut. Considerable yolk is still present at ES25, but the pigmentation pattern is largely established and scalation is well developed over all areas of the body. Scale pigmentation is similar to that of hatchlings and the skin is tough to cut. Long pointed claws occur both on the fingers and toes. The braincase is almost closed.

Light microscopy

Large parts of the epidermis consist of 2 layers varying in thickness from 4 to 8 μm in different body regions at ES13. Like the peridermis, the basal cells are very flat, with broad intercellular spaces and mitoses are common (Figs 2, 3). Some small areas, particularly in the head region, still consist of a single layer of ectoderm. No continuous basal membrane is visible under the epidermis. The dermal mesenchyme is very loose and most mesenchymal cells are homogenously distributed under the epidermis. Very few cytoplasmic arms from mesenchymal cells contact the epidermis.

A semiquantitative ratio of the number of peridermal cells that overlay basal epidermal cells in different skin areas was calculated by counting the basal cells beneath 30 peridermal cells along the epidermal surface in different body regions. There was an average of 2.8 basal cell per peridermal cell at ES13 in the head, ventral and dorsal areas. The PAS reaction showed that no glycogen is present in epidermal or dermal cells at this stage.

At ES16, the embryo has no melanogenic cells either in the dermis or epidermis. The epidermis is bilayered (thickness 8–14 μm depending on the body region) (Fig. 4) and there are few suprabasal cells. No glycogen is detectable by the PAS reaction. Mitotic

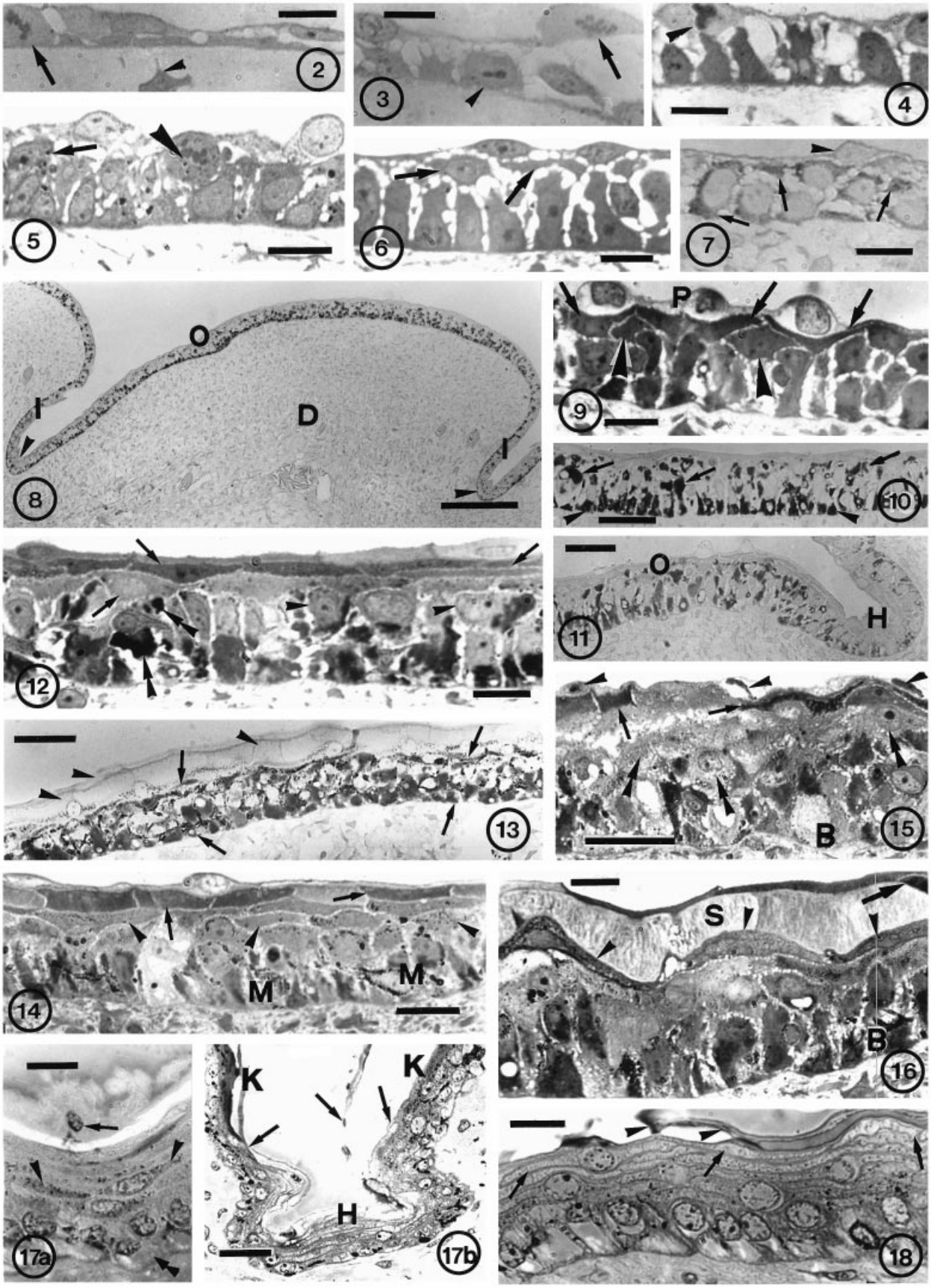

Figs 2–18. For legend see opposite.

cells are common in the epidermis and occasionally in the peridermis. There is an average of 3.3 basal cells per peridermal cell (trunk). Basal cells are irregular and not associated with a compact epithelium as broad extracellular spaces are still present. The shape of the cells of the basal layer varies from flat, as for the peridermis, to cuboidal. More frequent mesenchymal arms occur under the columnar epidermis, although dermal-epidermal contacts are not as numerous as in later stages.

At ES18, suprabasal cells are still scarce, although more common than in previous stages (Fig. 5) and basal cells become more columnar in different epidermal regions (thickness 12–18 μm depending on body region), particularly at the apex of the limbs where they form the apical ectodermal ridge. Mitoses are still seen along the flat epidermis of most body regions or in the initial undulated epidermis of the back and tail. This undulation foreshadows the formation of the first scales in these areas. Glycogen is generally absent from most epidermal and dermal cells, although a few peridermal and epidermal cells show small PAS positive clumps of glycogen. Occasional melanogenic cells are present in both the epidermis and dermis.

Most of the epidermis is still bilayered (thickness 14–25 μm depending on the region) at ES19–20, although occasional suprabasal cells are seen especially in the epidermis of the tail and back (Fig. 6). Most of basal cells are cuboidal or columnar and glycogen becomes visible, particularly in the undulated areas of the epidermis where scales are forming (Fig. 7). Peridermal cells, often containing diffuse glycogen throughout the cytoplasm, stretch to overlie 3.7 basal cells in skin of the trunk. The dermis starts to form a superficial dense and a deep reticular layer in most body areas other than the head and distal regions of limbs and tail. Scale morphogenesis in the dorsal caudal and trunk regions is advanced at this stage and the initial epithelial sheet has formed

Fig. 2. Light microscopic view of flat epidermis of two layers in the ventral trunk at ES13 with a mitosis (arrow) and sparce mesenchymal cells (arrowhead). Bar, 10 μm.

Fig. 3. Epidermis of the upper dorsal trunk consisting of cuboidal cells at ES16 showing a dividing cell in the epidermis (arrowhead) and peridermis (arrow). Bar, 10 μm.

Fig. 4. Bilayered epidermis of tail at ES18 featuring cylindrical basal cells and a dividing peridermal cell (arrowhead). Bar, 10 μm.

Fig. 5. Epidermis of hind limb at ES18 showing a suprabasal cell (arrow) and a dividing cell (arrowhead). Bar, 10 μm.

Fig. 6. Epidermis of tail at ES20 showing flat suprabasal cells (arrows) over columnar basal cells. Bar, 10 μm.

Fig. 7. Epidermis of lateral trunk at ES21 showing some glycogen accumulations (arrows) under the peridermis (arrowhead). PAS stain. Bar, 10 μm.

Fig. 8. Asymmetric tail scale at ES22 showing glycogen accumulated in most of epidermal cells along the outer scale surface (O) and reduced in those of the inner (I) and hinge regions (arrowheads). D, dermal core. PAS-stain. Bar, 50 μm.

Fig. 9. Epidermis of proximal tail at ES22 showing one flat sub-peridermal layer (arrows) beneath the pale peridermis (P), and a suprabasal layer (arrowheads). Bar, 10 μm.

Fig. 10. Epidermis of the outer surface of a tail scale at ES22 showing extensive glycogen accumulation in basal (arrowheads) and suprabasal (arrows) cells. PAS stain. Bar, 25 μm.

Fig. 11. Epidermis of lower back scale at ES22 showing the decrease in glycogen content from the outer surface (O) to the hinge region (H). PAS stain. Bar, 25 μm.

Fig. 12. Epidermis of the outer surface of a back scale at ES23 with 2 flat sub-peridermal layers (arrows) located above the suprabasal layer (arrowheads). Pigmented melanocytes are present (double arrowheads). Bar, 25 μm.

Fig. 13. Epidermis of the outer surface of a dorsal proximal scale at ES23 showing the high content of glycogen in basal and suprabasal cells (between arrows). Glycogen disappears in the outer subperidermal and peridermal layers (arrowheads). PAS-stain. Bar, 25 μm.

Fig. 14. Epidermis of the outer surface of a scale of proximal hind limb at ES24 showing 3 sub-peridermal layers, in the more external of which dark cells are visible (arrows). Arrowheads on presumptive β-cells. M, melanocytes among basal and suprabasal cells. Bar, 25 μm.

Fig. 15. Epidermis of outer surface of belly scale at ES24 showing dark (pyknotic) nuclei in the peridermis (arrowheads), shrunken dark cells in the first subperidermal layer (arrows), paler presumptive β-cells (double arrowheads). B, basal layer. Bar, 20 μm.

Fig. 16. Portion of epidermis of outer surface of flank scale at ES24. The flat peridermal layer shows a pyknotic nucleus (arrow). The pale subperidermal layer (S) contains fibrous material. Arrowheads indicate the first layer of differentiating β-cells which are toluidinophilic. B, basal layer. Bar, 10 μm.

Fig. 17(*a*). A portion of epidermis of outer surface of a ventral scale at ES25 showing detachment of the flat embryonic epidermis (the arrow indicates a dark nucleus) from the pigmented (arrowheads) β-keratinised layers. Double arrowhead, basal layer. Bar, 10 μm.

Fig. 17(*b*). Close-up of forelimb epidermis at ES25 showing that the β-keratin layer (K) disappears (arrows) in the hinge region (H). Bar, 25 μm.

Fig. 18. Longitudinal section of epidermis of outer surface of proximal forelimb scale at ES25 showing the stratification of β-cells that become flatter and paler (arrows) in the more external layers. The flat embryonic epidermis (arrowheads) is partially detached. Bar, 10 μm.

into definite, symmetric bumps. Glycogen increases in the basal cells and in the peridermis of the bumps. The epidermis and dermis are the same as at ES18 and glycogen is absent in nonscaled areas (ventral, limbs and head). Cells located in the epidermal bumps, the future outer scale surface, at least in their central part, are often taller and with more suprabasal cells than in the concave part between bumps, the future hinge and inner scale regions. There are few pigment cells.

At ES21, basal epidermal stratification (thickness 15–25 μm, depending on the body region) more or less resembles that of the previous stage, but glycogen clumps occur in basal and peridermal cells, particularly where more stratification is visible. Glycogen is dramatically increased in these cells compared with earlier stages, but is also present, although in lower quantity, in the periderm and epidermal cells of the future hinge region. This appearence remains through ES22 and 23 (Fig. 8). In the forming hinge regions, particularly in dorsal or caudal asymmetric scales, glycogen decreases or disappears in the cuboidal epithelium. No glycogen is present in the epidermis of the limbs and head where the epidermis is often pseudostratified and resembles that found in the previous embryonic stage. The dermis consists of 3 layers at this stage, since a reticulate connective tissue (subcutis; Lange 1931) appears beneath the dense and loose superficial layers in many body regions. Pigment cells are still rare.

A few suprabasal cells are present in the digits and distal epidermis of limbs, head, and flank at ES22, while a flat subperidermal layer is sometimes seen above the suprabasal layer in scales of the tail, back, belly and neck where the epidermis is often 4 layers thick (Fig. 9). The thickness of the epidermis is therefore quite variable (15–30 μm) over different body regions. The peridermal cells now overlie 7.5 (tail) and 8.5 (limb) basal cells and the less numerous peridermal cells are often vacuolated, thin and stretched over columnar basal cells. Glycogen is present in both basal and suprabasal cells along the scales, including in the hinge regions (Figs 8, 10, 11). Pigment cells are still sparse in the skin.

At ES23, the asymmetric plate-like scales (mostly of the tail, back, belly and less frequently in other body regions) or in tail verticils (the elevated asymmetric scales of the double and single row in the tail of crocodilians) (Brazaitis, 1987) and the basal cells of the outer (dorsal) scale surface contain columnar cells, while the hinge regions often contain cuboidal cells. Peridermal cells are more stretched in the region of the outer surface of the plate-like scales than in or near the hinge regions. Some peridermal cells also appear vacuolated and flake off. The peridermal cells now overlie 9.8 (tail), 8.9 (back) and 10.0 (neck) basal cells, and the peridermal cells are extremely flat (the coverage is, however, sometimes interrupted and some cells are missing). Basal cells maintain their columnar shape and 1–2 flat suprabasal cells are present, commonly as 2 layers in the tail, neck, back and belly scales, and generally as one layer in the limb, digits, head and gular scales (Fig. 12). The thickness of the epidermis therefore varies in different body regions (18–35 μm). The first appearance of a layer of β-keratin beneath the subperidermis occurs in a few cells located in the central portion of the outer scale surface of the back, tail, neck and ventral scales, but not in scales of limbs, digits, throat and head at this embryonic stage. The suprabasal layer is generally paler than the uppermost 1–2 subperidermal layers. Glycogen is very abundant in both basal and suprabasal cells of the outer scale surface, sparse in hinge regions, and often absent from the peridermis (Fig. 13). Pigment cells are present for the first time in the epidermis of different regions and they are more frequent in some areas, probably the pigmented bands (Fig. 1*C*). There is little glycogen in the epidermis of the digits and head, and the tissue resembles that of tail, belly and dorsal regions at ES21–22. Few or rare irregularly-shaped pigment cells are present in the external dermis but are more common at this stage in the deep reticular layer of the dermis. The dermis is similar to the previous stage, but contains more numerous and large extracellular fibrils.

At ES24, the epidermis becomes more heavily pigmented and the banding pattern is well established (Fig. 1*D*). The basal layer is still composed of columnar cells on the outer surfaces of the scales of the dorsum, tail, neck (Fig. 14). The epidermis varies in thickness from 20 to 40 μm. More cuboidal-shaped basal cells occur in the hinge region of scales, although in the tuberculate scale (bump-like) of the flank, gular and neck regions, the epidermal thickness is more uniform. Glycogen is present in most basal cells and in the first and second suprabasal layers of the outer scale surface, decreases in the hinge regions, and is absent from the peridermis and upper flat subperidermal layers. Two (flank, gular, limb-digits, flank), or more frequently 3 (back, tail, neck, belly), suprabasal flat layers lie above the columnar basal layer. In the belly, tail and dorsal scales, there are 3 suprabasal layers towards the centre of the scale and 2 towards the hinge region. The external flat peridermis is more frequently vacuolated with pyknotic (dark) nuclei (Figs 15, 16) and in some areas is missing or desquamating. The peridermal cells now overlie

12.7 (dorsal), 11.3 (flank), 13.2 (neck), 17.4 (ventral), 15.5 (limb) basal cells. Also the first and second subperidermal layers are quite flat and dark areas are visible in their cytoplasm (Figs 15, 16). Melanocytes are located among basal cells and their arms extend among suprabasal cells but not into the first subperidermal layers. There are few pigment cells in the dermis at this stage.

β-cells with a dark outline are forming over the paler pre-β-layer beneath 1–2 subperidermal layers of the outer scale surface in dorsal, tail, neck and ventral areas (Fig. 16). Maturing β-cells show a fine network of toluidine positive filaments at the limit of resolution of the light microscope, and possibly some lipid droplets or vesicles. Pre-β-cells in the suprabasal layer are less toluidinophilic than those of the external layers and show a pigmented cytoplasm. At this stage, a β-keratin layer is also forming in many scales of the gular, flank and neck regions, although a darker β-keratin layer is not present under the subperidermis of all scales in these regions and the epidermal histology resembles that of ES23. A β-layer has not yet formed in scales of the head, digits and distal limb regions, where the epidermis still resembles that of ES22–23. Dermal fibrils in the intermediate compact layer become thicker and denser as they increase in number.

At ES25 basal cells are cylindrical to cuboidal in the outer scale surface and still contain clumps of glycogen. There is much less glycogen in the suprabasal layer and virtually none in the uppermost layers. All epidermal areas have 2–3 suprabasal layers with fusiform cells beneath 4–8 (more numerous in dorsal, tail and ventral scales than in the remaining) extremely flat external suprabasal cells (Figs 17*a*, 18). Depending on the body region, and even along the outer surface of the same scale, the epidermal thickness varies from 25 to 50 μm and is only 10 to 12 μm in the hinge region of scales (Fig. 17*b*). The flattening cells show a slight toluidinophilic outline and granular content, typical of β-cells, but their boundaries remain visible. Many granules of pigment that are continuous with arms of epidermal melanocytes are located within these flat keratinising cells. The β-layer thins between the outer scale surface and the hinge region, where it is absent (Fig. 17*b*). The superficial cells contain lipid droplets. Often the more external 1–2 β-keratin layers are pale or toluidine negative and represent the first mature β-keratin layer (Fig. 18). The outermost embryonic layers (periderm and 1 or 2 subperidermal layers), often have very dark cells and make a thin cornified layer containing pyknotic nuclei (Fig. 17*a*). The embryonic epidermis at ES25 often appears desquamating and easily splits during sectioning (Fig. 17*a*). Dermal melanocytes are more abundant than in early stages, but are less abundant than epidermal melanocytes.

Electron microscopy

From ES16 to ES18, the cytoplasm of peridermal and epidermal cells contains the usual cell organelles, occasional lipid droplets and very little glycogen (Figs 19, 20). The cytoskeleton is limited and is represented by occasional microtubules and isolated intermediate filaments. Sparse 0.05–0.1 μm diameter, electron-dense granules, resembling previously described mucus granules (Parakkal & Alexander, 1972; Landmann, 1986), occur in the peridermis (Fig. 19 inset). These mucus granules derived from the Golgi apparatus, are occasionally fused to the external plasmalemma, suggesting that they discharge their contents into the external space. Other small vesicles are present in the cytoplasm, while a few micropinocytotic vesicles occur on the external surface where microvilli are present. More frequently, micropinocytotic vesicles are present in the cytoplasm facing the basement membrane, where no hemidesmosomes are seen (Fig. 20).

The intercellular spaces are broad and irregular and there are many thin microvillar projections between adjacent basal cells and between basal and peridermal cells (Fig. 19). Few desmosomal junctions are visible between epidermal cells and between epidermal and peridermal cells, while desmosomes are common between peridermal cells. Desmosomes joining epidermal cells are more frequent at ES18 than ES16, although broad intercellular spaces still persist. At these stages the basement membrane is composed of a lamina densa underlain by a few collagen fibrils (Fig. 20).

At ES19–20, occasional small and sparse bundles of intermediate (keratin) filaments are visible in the few suprabasal cells (Fig. 21). Desmosomes between epidermal cells and with the periderm are common and extracellular spaces are reduced. Collagen fibrils increase under the basement membrane at ES19.

At ES21, keratin bundles are more common in epidermal cells and are also visible in basal cells although they are generally less numerous than in the suprabasal cells. Glycogen particles are diffuse or sometimes aggregated into larger masses. Hemidesmosomes are still rare at this stage.

Intercellular spaces are reduced at ES22–23 among both the columnar basal cells and suprabasal cells (Figs 22, 23). The number of glycogen particles increases throughout the peridermal and epidermal

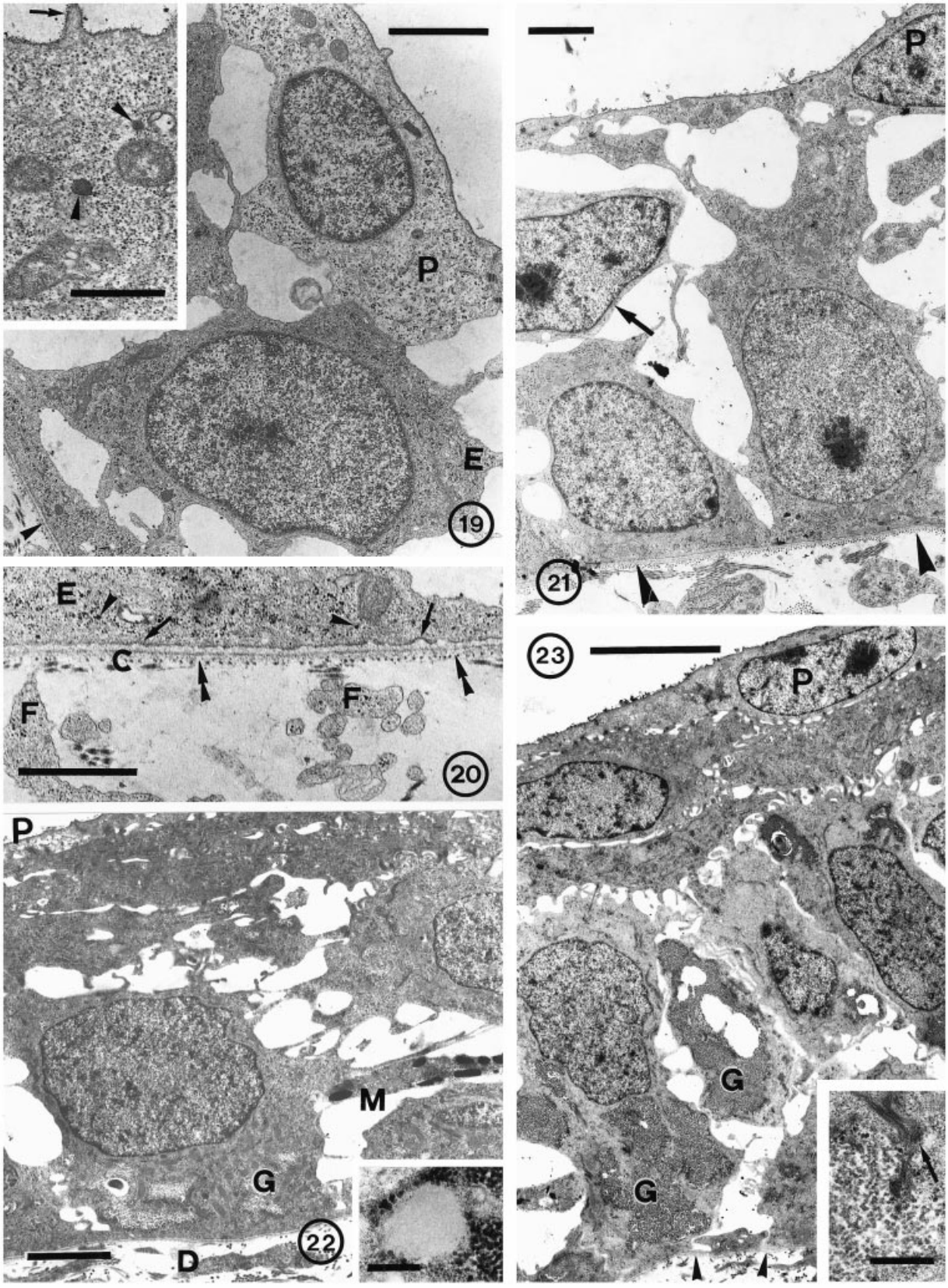

Figs 19–23. For legend see opposite.

cells, particularly in the basal and columnar pseudostratified layer of the outer scale surface. Among glycogen clumps (1–4 μm in diameter), lipid droplets sometimes reaching 1–2 μm in diameter are more numerous than before (Fig. 22). Like glycogen, lipid droplets tend to disappear in cells above the first suprabasal layer, particularly after ES22. Some peridermal cells appear pale, partially detached from the underlying layer, and sometimes they flake off. Thus it is the first subperidermal layer that remains on the surface. In the flattening cells beneath the pale peridermis, small clumps of glycogen are present together with single or bundles of intermediate filaments which are often oriented horizontally along the sagittal plane. Hemidesmosomes are more frequently seen from ES22 onwards.

At ES23, the first few melanocytes colonise the basal and suprabasal layers. The first flattening subperidermal cells contain 25–35 nm diameter coarse filaments which start to aggregate into a larger meshwork of reticulate bodies (Fig. 24). The intermediate filament meshwork contacts the coarse filaments within reticulate bodies. The reticulate bodies tend to be absent from the suprabasal cells of the hinge regions. Larger glycogen clumps occur among numerous bundles of keratin filaments in the second and, when present, third subperidermal layers. Sparse rough endoplasmic reticulum, mitochondria and occasional glycogen particles, with some blebbing vesicles from the Golgi apparatus and smooth endoplasmic reticulum, occur in these cells (Figs 24, 25). The number of coarse filaments increases and they fill large parts of the periderm and the first 1 or 2 subperidermal layers (Figs 25, 26). Subperidermal cells are often more electron dense and contain numerous 0.1–0.25 μm diameter mucus-like granules in the external cytoplasm not occupied by the coarse filament meshwork (Figs 25, 26). The mucus-like granules are produced in the Golgi apparatus (Fig. 27) and some of them show concentric or parallel lamellation, with a space of 3.6–4.5 nm between lamellae (Fig. 28). The lamellar bodies and mucus-like granules accumulate and discharge their content into the extracellular space, especially on the external side. Pigmentation is intense in some epidermal areas in the second and particularly third subperidermal layers. Most dermal melanophores show no ultrastructural differences from epidermal melanocytes.

At ES24, many desmosomes link the subperidermal layers. The periderm, particularly that over the outer scale surface, is often swollen, vacuolated, electron-pale and sometimes even detached from the subperiderm (Fig. 29). Desmosomes appear incomplete between the periderm and subperiderm in some areas, without desmosomal plaques in the cytoplasm, suggesting desmosomal degradation (Allen & Potten, 1975; Menon et al. 1992). However, desmosomes are still present between some peridermal and subperidermal cells. Nuclei of 1–2 subperidermal layers progressively accumulate clumps of heterochromatin and become dark. The layer beneath the subperidermis has no coarse filaments but contains sparse vesicles of smooth endoplasmic reticulum or vacuoles, lipid droplets, free or small clumps of glycogen particles, and some melanosomes. Some of the bundles of filaments inside their cytoplasm have denser spots which indicate that these are early differentiating β-keratin cells (Fig. 30). In tail, back and belly scales, differentiating β-cells in the layer underneath the subperidermis contain large bundles of irregularly-oriented and dark keratin filaments. The bundles generally increase from the cell periphery to the perinuclear areas (Figs 30, 31). The ultrastructural analysis shows that the first keratin filaments are associated with ribosomes and that the bundles rapidly increase in diameter. Vesicles, or even vacuoles, and lipid droplets among β-keratin bundles, are often associated with glycogen (Figs 32, 33). Mitochondria show few cristae and become paler or disappear as keratin filament bundles accumulate.

Fig. 19. Sagittal electron microscopic view of bilayered epidermis from the belly at ES16 showing diffuse dot-like glycogen particles (darker) mixed with ribosomes (paler and smaller) in both peridermis (P) and basal (E) cells. Arrowhead on the basement membrane. Broad extracellular spaces and thin cytoplasmic arms joining the cells are seen. Bar, 2 μm. The inset (Bar, 1 μm) details the peridermal surface with a microvillus (arrow) and two dark mucous-like granules (arrowheads).

Fig. 20. Sagittal view of basal cytoplasm of trunk epidermal cell (E) at ES16 with few glycogen particles (arrowheads), pinocytotic vesicles (arrows). Collagen fibrils (C) and arms of dermal fibroblasts (F) contact the basement membrane (double arrowheads). Bar, 1 μm.

Fig. 21. Tail epidermis at ES20 showing a suprabasal cell (arrow) and broad intercellular spaces. Arrowheads on the basement membrane with cross sectioned collagen fibrils. P, peridermis. Bar, 2 μm.

Fig. 22. Portion of caudal inner scale epidermis at ES22 showing 2 suprabasal cell layers above the cuboidal basal layer with glycogen clumps (G). P, peridermis. M, melanocyte arm. D, long dermal fibroblast arms under the basement membrane. Bar, 2 μm. The inset (Bar, 250 nm) shows a lipid droplet surrounded by glycogen particles.

Fig. 23. Outer scale peridermis of tail scale with 2 suprabasal cells under the peridermis (P) at ES22. Columnar basal cells contain large clumps of glycogen (G) and filament bundles (arrow in the inset, Bar, 0.5 μm). Arrowheads on basement membrane. Bar, 5 μm.

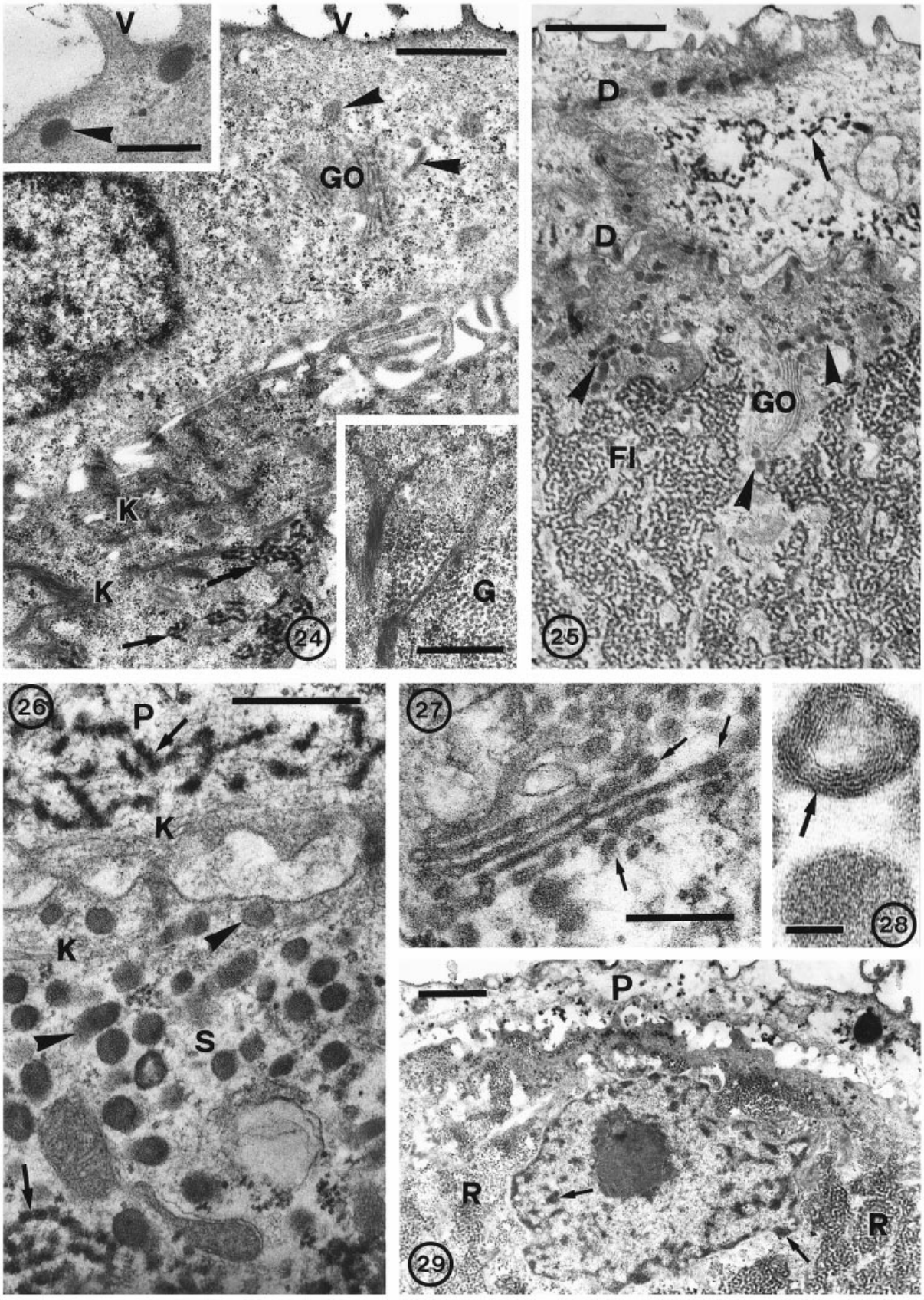

Figs 24–29. For legend see opposite.

Nuclei of differentiating β-cells progressively accumulate heterochromatin clumps. Denser areas of β-keratin material appear over previously formed intermediate filament bundles as differentiation proceeds (Fig. 31 upper inset). Intermediate filament bundles merge to fill the cytoplasm (Figs 31, 34), but no massive β-keratin bundles were observed at ES24. The ultrastructural analysis at high magnification ($\times$150000–300000) of the keratin bundles shows 2–3 nm thick electron-lucent fibrils embedded in an irregular electron dense matrix (Fig. 31 lower inset). Suprabasal cells beneath differentiating β-cells contain some vesicles, sparse ribosomes, small clumps of glycogen and occasional small keratin bundles without the denser spots.

A schematic summary of stratification and differentiation in alligator epidermis is presented in Figure 35.

DISCUSSION

Peridermis and embryonic epidermis

The simple epidermis at ES13 is a loose epithelium where the shape and protrusions of the cells suggest that they can undergo limited movement within the immature tissue. The absence of an extensive keratin cytoskeleton, and the lack of tonofilaments converging onto desmosomes, probably impede the cohesiveness of the epithelium at ES13–16. This structure allows a high rate of cell multiplication and the superficial expansion of the epidermis with embryonic growth, but does not provide for stratification. The accumulation of keratin bundles at ES18 allows epidermal stratification but it is not until ES20 that a suprabasal layer is present. Keratin bundles are also associated with the accumulation of glycogen, a phenomenon that precedes β-keratin production (Matulionis, 1970; Alibardi, 1998*b*).

The embryonic epidermis, represented by the peridermis and the first 1 or 2 subperidermal layers in the alligator, is similar to that of lizards (Dhouailly & Maderson, 1984; Alibardi, 1998*a*, *b*; Alibardi & Thompson, 1999*a*). In contrast, the embryonic epidermis is made of 4–5 layers in the turtle *Emydura macquarii* (Alibardi & Thompson, 1999*b*). All these embryonic epidermises resemble the mucus-secreting epidermis of fish and amphibians (Budz & Larsen, 1975; Matoltsy & Bereiter-Hahn, 1986; Matoltsy, 1987). The progressive increase in periderm to basal cell ratio is indicative of the expansion of the epidermis and loss of peridermal cells during late embryonic stages. The peridermal swelling and vacuolated degeneration lead to sloughing of these cells during embryonic life before hatching, as in skin of birds (Parakkal & Matoltsy, 1968; Alibardi, 2000).

The mucus granules in alligator skin coexist with lamellar bodies, as in the embryonic epidermis of the turtle *Emydura macquarii* (Alibardi & Thompson, 1999*b*). It is possible that during the evolution of amniotes, the primitive Golgi apparatus that produces mucus or glycoproteins in amphibians produced new lipids or glycolipids-waxes which are more effective than mucus as a barrier to water loss in a terrestrial environment (Lillywhite & Maderson, 1982; Matoltsy, 1987; Menon et al. 1986, 1996). Both glycoproteins in mucus bodies and glycolipids in lamellar bodies contain monosaccaride/sugar residues (Landmann, 1980; Menon et al. 1986).

Another addition to the amphibian epidermis in amniotes was the appearance of aggregations of coarse filaments for initial cornification. As in other sauropsids, the cornification of the peridermis and embryonic epidermis from ES24 onwards in the alligator results from the formation of 25–35 nm coarse filaments into a network of reticulate bodies that incorporate keratin filaments. The network of intermediate filaments of keratin aggregate with the

Fig. 24. Epidermis of the forelimb at ES23 showing the pale peridermis with surface microvilli (V), sparse glycogen and some mucous granules (arrowheads) produced in the Golgi apparatus (GO), as better illustrated in the upper inset (Bar, 250 nm). Bundles of keratin (K) and the initial aggregation of coarse filaments (arrows) among diffuse glycogen particles (G in the lower inset, Bar, 0.5 μm) are present in the differentiating first sub-peridermal layer. Bar, 1 μm.

Fig. 25. Epidermis of the tail at ES23 showing the external pale peridermis with few coarse filaments (arrow). The first subperidermal layer contain large aggregations of coarse filaments (FI), superficially Golgi bodies (GO) and mucous granules (arrowheads), but lacks glycogen. D, desmosomes. Bar, 1 μm.

Fig. 26. Higher magnification of epidermis from the lower back at ES23 showing adjacent to peridermal (P) and sub-peridermal (S) cells. Intermediate keratin filaments (K) are distributed among coarse filaments (arrows). Arrowheads on mucus-like granules, some close to the plasmalemma. Bar, 400 nm.

Fig. 27. Golgi apparatus of subperidermal layer of epidermis from the lower back at ES23 with blebbing mucus-like granules (arrows). Bar, 200 nm.

Fig. 28. High magnification of two mucous-like granules in lower back subperidermal cell, one of which (arrow) is lamellate. Bar, 50 nm.

Fig. 29. Epidermis of the tail at ES24 showing clumping of coarse filaments into large reticulate bodies (R) and clumping of nuclear heterochromatin (arrows) in the subperidermal layer. The pale peridermis cytoplasm (P) is swollen. Bar, 1 μm.

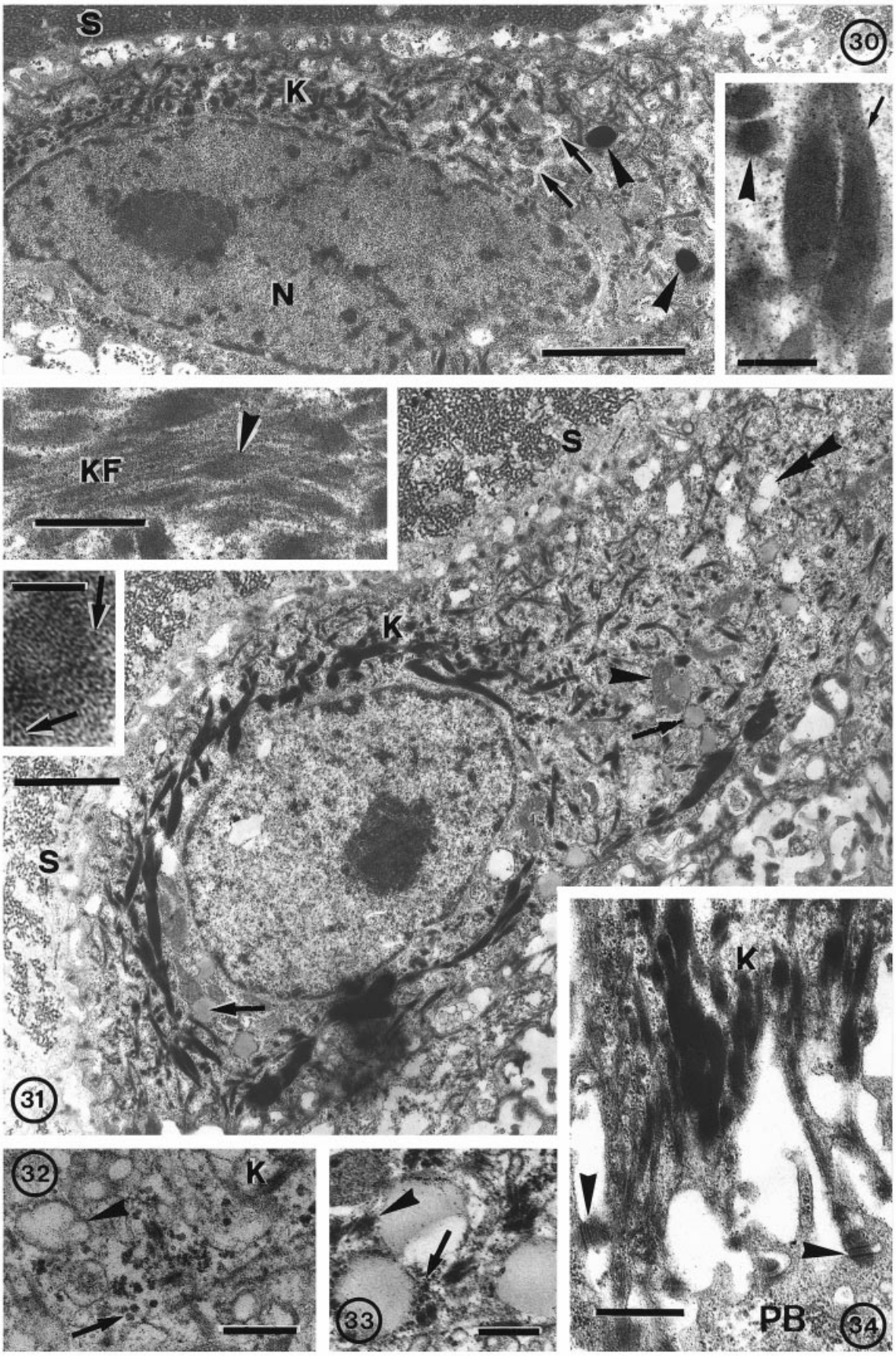

Figs 30–34. For legend see opposite.

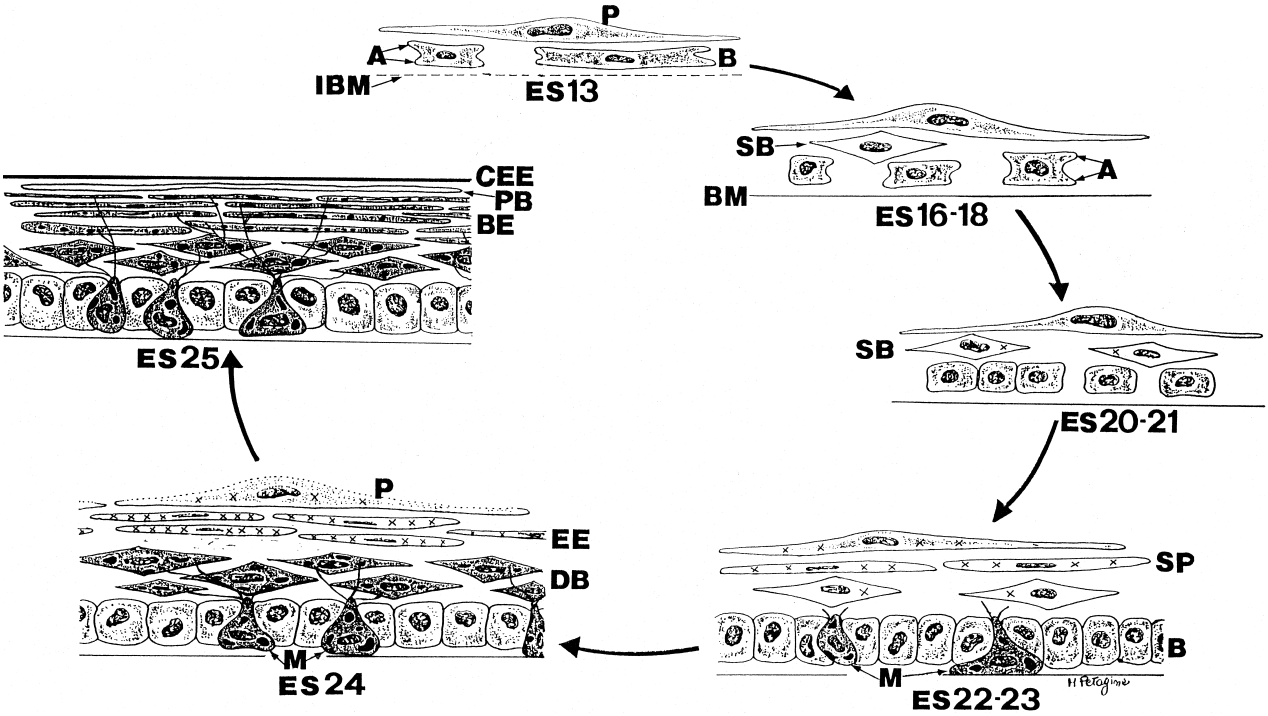

Fig. 35. Schematic drawing summarising the phases of epidermal differentiation in embryonic alligators. A, cytoplasmic arms. B, basal cells BE, beta differentiating cells. BM, basement membrane. CEE, compact embryonic epidermis. DB, differentiating beta-cells. EE, embryonic epidermis (peridermis + subperidermis). ES, embryonic stages. IBM, incomplete basement membrane. M, melanocytes with their arms. P, peridermis. PB, pale compact beta cells. SB, suprabasal cells. SP, subperidermal cells. The crosses (×) in subperidermal cells represent reticulate bodies.

reticulate bodies and eventually, at ES25, condense to provide the final cornification. The molecular nature of the coarse filaments, representing an amniote cytoskeletal component not yet described in anamniotes, is presently unknown. They may represent a form of embryonic keratohyalin or a keratohyalin precursor (Matulionis, 1970). Similar organelles, associated with a more or less dense matrix, have been described in the embryonic or mucus-secreting epidermis of birds (Mottet & Jensen, 1968; Parakkal & Matoltsy, 1968; Matulionis, 1970; Sawyer et al. 1986; Alibardi, 2000), and mammals (Bonneville, 1968; Du Brul, 1972; Fukuyama & Epstein, 1973; Hardy et al. 1978). The roundish granules, resembling embryonic keratohyalin, consist of a dense matrix containing coarse filaments and they mature into typical keratohyalin as the embryo approaches birth (Bonneville, 1968).

Changes in the intercellular junctions

The small number of desmosomes during early stages of epidermal formation (ES16–18) is rapidly increased from ES20 onwards, and is associated with an increase

Fig. 30. Epidermis of forelimb with differentiating β-cell underneath condensed subperidermal cell (S) at ES24. Numerous keratin bundle filaments (K) are present in the uppermost cytoplasm but are reduced in the middle-lower cytoplasm in favour of ribosomes and cisternae of rough endoplasmic reticulum (arrows). Two melanosomes are visible (arrowheads). The dark nucleus (N) shows heterochromatin clumps. The inset at higher magnification (Bar, 200 nm) features cross (arrowhead) and longitudinally sectioned (arrow) β-keratin bundles. Bar, 2 μm.

Fig. 31. More advanced differentiating β-cell at ES24 in epidermis of the forelimb with numerous, irregularly distributed, small and large, merging bundles of keratin filaments (K), especially around the nucleus. Lipid droplets (arrows), vacuoles (double arrowhead) and few mitochondria (arrowhead) are visible. Reticulate bodies are seen in subperidermal cell (S). The upper inset (bar, 200 nm) shows the formation of darker points (arrowhead) of deposition or compaction of β-keratin (matrix) over a fibrous keratin framework (KF). The lower inset (bar, 40 nm) shows the electron-lucid β-keratin fibrils (arrows). Bar, 2 μm.

Fig. 32. Detail of the cytoplasm of differentiating β-cell of epidermis of the lower back at ES24 with forming lipid-like vesicles from smaller smooth endoplasmic reticulum vesicles (arrowhead). Few glycogen particles (arrow) and initial keratin fibrils (K) are present. Bar, 250 nm.

Fig. 33. Detail of lipid droplets associated with glycogen (arrow) and keratin (arrowhead) in β-differentiating cell of proximal forelimb at ES24. Bar, 250 nm.

Fig. 34. Detail of passage region between differentiating β-keratin cell of proximal forelimb at ES24 with large β-keratin filament bundles (K) and a pre-β-cell (PB) with no filaments. Arrowheads on 2 desmosomes. Bar, 0.5 μm.

of epidermal cohesiveness and cell stratification. A small number of intercellular contacts also is typical of the early stages (embryonic to early fetal) of epidermal differentiation in both avian and mammalian epidermis (Parakkal & Matoltsy, 1968; Lyne & Hollis, 1972). The ultrastructural differentiation of desmosomes (and hemidesmosomes) follows that described in the mammalian epidermis: initially the dense plaques form, then the intercellular dense matrix and plaque, and eventually the tonofilaments converge into the cytoplasmic dense plaques (Briggaman & Wheeler, 1975; Weiss & Zelickson, 1975*a–c*). However, with the formation of the β-layer underneath the embryonic epidermis many desmosomes between the peridermis and the first subperidermal layer appear to degrade in both the extracellular and intracellular plaques, as occurs in the sloughing keratinocytes of amphibian, snake and mammalian epidermis (Allen & Potten, 1975; Budz & Larsen, 1975; Landmann, 1979; Menon et al. 1992). With the differentiation of β-cells, instead of converging into desmosomes, the intracellular tonofilaments are incorporated into the β-keratin bundles and the intracellular plaques disappear. As a consequence the primary anchoring function of desmosomes is lost from ES23, and the sloughing of the peridermis initiates.

Epidermal differentiation

Stratification of the epidermis occurs earlier in the caudal, dorsal and ventral areas than in the neck, flank, throat and especially the limbs, digits, and head. At ES20–21, keratin bundles form in suprabasal and basal cells indicating a form of keratin accumulation that precedes the deposition of β-keratin in the presumptive β-cells produced from ES23 (dorsal, tail and ventral skin) or ES24 (most of remaining areas) onwards. The formation of cells with a dark outline at ES24 indicates that larger bundles of β-keratin are forming. At ES25, when the embryo looks like a small version of the hatchling (Ferguson, 1985, 1987), stratification of β-cells is present over all epidermal areas but the keratinised layer is slightly thicker (and tougher) in the dorsal, ventral and tail skin than elsewhere.

The differentiation of β-cells produces thin elements that do not merge into a syncytium as do those of lepidosaurs, but maintain the cell boundaries seen in some turtles and *Sphenodon* (Alexander, 1970; Parakkal & Alexander, 1972; Landmann, 1986; Maderson et al. 1998; Alibardi & Thompson, 1999*b*). The final differentiation of embryonic and β-keratinising epidermal cells is characterised by the darkening of the nucleus which becomes pyknotic, as it is in lizards (Alibardi, 1998*b*).

Glycogen increases in epidermal cells of the basal and suprabasal layers of alligator embryos where intense cell proliferation and the precursors of β-keratin are present, as it does in the embryonic epidermis of lizards (Alibardi, 1998*b*), snakes (Alibardi, personal observations), and birds (Matulionis, 1970; Alibardi, 2000). Glycogen is often associated with lipids, which may be the main source of energy for keratin synthesis, as in turtles (Matoltsy & Huszar, 1972; Alibardi & Thompson, 1999*b*) and some lizards (Alibardi & Thompson, 1999*a*). In rapidly metabolising epidermal cells, glycogen can be converted into glucose to be used for lipogenesis (Freinkel, 1991), or used as a rich source of metabolic energy for keratin production. The more osmiophilic lipid droplets probably contain more unsaturated lipids than the pale vacuoles, suggesting that most electron-pale lipid droplets contain saturated lipids. In fact the electron density of lipid vacuoles may decrease when more saturated lipids (glycolipids, waxes) are accumulated, as in epidermal cells of birds (Menon et al. 1986, 1996; Alibardi, 2000). Other lipid droplets may be derived from mitochondria, as observed in the turtle *Emydura macquarii* (Alibardi & Thompson, 1999*b*) and birds (Frazer et al. 1972). These lipids seem to be more prevalent than keratin in the hinge regions of alligator scales.

The depletion of glycogen and lipids is associated with cell proliferation and keratin synthesis by ribosomes. Although not quantified in the present study, the number of ribosomes rapidly decreases in keratin accumulating cells, as in the chick (Matulionis, 1970; Kemp et al. 1974). Contrary to earlier reports (Landmann, 1979, 1986), embryonic alligators resemble lizards and turtles (Alibardi, 1998*a*, *b*; Alibardi & Thompson, 1999*b*) where no elaboration of β-keratin takes place in the Golgi apparatus of β-cells. Instead the Golgi apparatus and the smooth endoplasmic reticulum seem to be associated with the production of lipid vesicles, probably an earlier characteristic of differentiating β-keratin cells, as in the β-keratinising cells of the zebrafinch (Alibardi, 2000).

The β-keratin seen in the 2–3 nm thick electron-lucent fibrils (Fig. 31) is deposited on small bundles of α-keratin filaments, as previously seen in β-cells of scutate scales, and epidermis of the beak and tongue of chickens (Sawyer et al. 1974; Carver & Sawyer, 1988, 1989; Shames et al. 1988, 1989, 1991). Although a specific ultrastructural study has not been done, it is

likely that a similar process takes place in avian feather cells (Haake et al. 1984; Mayer & Baumgartner, 1998). β-keratin molecules progressively combine into larger bundles which have an irregular orientation within the cells. Bundles of β-keratin filaments are oriented along the main cell axis only in barbule, barb and calamus cells of the feathers (Matulionis, 1970; Frazer et al. 1972; Kemp et al. 1974; Bowers & Brumbaugh, 1978; Alibardi, 2000). The different orientation of β-keratin filament bundles in the alligator and birds is probably associated with changes in the shape of β-cells which form flat scales in alligators. Instead, the orientation of β-fibrils along the axis of β-cells probably contributes to the formation of the cylindrical shapes of barbs and barbules of feathers.

The mechanism of formation of β-keratin bundles in turtles, snakes, *Sphenodon*, and lizards is slightly different from that seen in birds and the alligator. In turtles and lepidosaurs, β-keratin packing is derived from the initial association of α-keratin filaments to roundish β-keratin packets representing a matrix material (Alexander & Parakkal, 1969; Alexander, 1970; Roth & Jones, 1970; Maderson et al. 1972, 1998; Landmann, 1979, 1986; Alibardi, 1998*a*, *b*, *c*; Alibardi & Thompson, 1999*a*, *b*). This electron-dense matrix material surrounds the keratin filaments and produces a pattern of electron-lucent 3 nm thick fibrils, termed the β-keratin pattern (Baden & Maderson, 1970; Frazer et al. 1972; Baden et al. 1974; Landmann, 1979, 1986). After the beginning of fusion of β-keratin packets in lepidosaurs and turtles, β-keratinisation is similar to that of the alligator and birds. The packing and compaction of β-keratin after ES24 in embryonic alligators is probably responsible for the loss of staining with toluidine blue or electron-density of the external keratinised layers, as observed both at the light and electron microscopic level for other reptiles (Baden & Maderson, 1970; Alibardi & Thompson, 1999*b*).

The cytological process of β-keratinisation in reptiles and birds resembles that observed during hard keratinisation in mammals, e.g. in nails and hair (Hashimoto, 1971; Marshall et al. 1991). There is no keratohyalin present in prekeratinising cells of nails and hair in mammals and large bundles of keratin (α-keratin with electron-lucent fibrils of 8–10 nm in thickness) eventually merge to produce a variegated but compact keratin layer. While β-keratin of reptiles and birds is hard and inextensible, in mammals these properties are conferred by the high sulphur/tyrosine matrix proteins added to keratin bundles (Marshall et al. 1991).

Barrier formation in reptiles as compared with that of other amniotes

The formation of the epidermal barrier against water loss, and as mechanical and microbic protection, prepares the embryo to survive in the terrestrial environment. In the alligator, this process begins from ES23 with the initial production of the first β-cells, which represent the future and permanent stratum corneum in adults (Spearman & Riley, 1969; Alexander, 1970; Landmann, 1986). The maturation of the epidermis in alligator embryos is regional, and it spreads from the dorsocaudal areas to lateroventral and cephalic areas. This gradient in the formation of the epidermal barrier has been found also in rodents among mammals (Hardman et al. 1998).

During embryogenesis in mammals the epidermis passes through 4 main periods (Lyne & Hollis, 1972; Weiss & Zelickson, 1975*a*, *b*, *c*; Dale et al. 1985; Dale & Holbrook, 1987). In the first (embryonic period), no stratification occurs. In the second (fetal) period, stratification takes place but no keratinisation occurs, so no epidermal barrier is yet present. The 2 first periods are also recognisable in the developing alligator skin, as well as in the other reptiles (Dhouailly & Maderson, 1984; Alibardi, 1998*a*, *b*; Alibardi & Thompson, 1999*a*).

A stratum corneum forms above a stratum intermedium in the last 2 (follicular keratinisation and interfollicular keratinisation) periods of epidermal development in mammals, where a transition between embryonic and adult epidermis takes place (Bonneville, 1968; Du Brul, 1972; Lyne & Hollis, 1972; Dale et al. 1985; Hardman et al. 1998). In the stratum intermedium, where the barrier is not completed, keratohyalin granules often show an heterogenous content, and multilamellar bodies and intercellular lipids are still scarce (Boneville, 1968; Du Brul, 1972; Lyne & Hollis, 1972; Fukuyama & Epstein, 1973; Weiss & Zelickson, 1975*b*, *c*; Hardy et al. 1978; Hardman et al. 1998). A stratum intermedium is also formed during embryogenesis of apteria epidermis in birds (Mottet & Jensen, 1968; Parakkal & Matoltsy, 1968; Spearman & Hardy, 1985) before the lipid-rich stratum corneum is formed (Menon et al. 1986, 1996).

In mammals, the stratum corneum with its intercellular lipid matrix functions as a barrier against water loss. This role seems to be taken over by lipid-rich β-cells in crocodilians, where no lamellar bodies are known, although this water-barrier is not as effective as in mammalian epidermis. A similar function is also evident for lipids in β-cells of feathers (Alibardi, 2000). Since intercellular spaces still remain

among β-cells in alligators (as in turtles and in *Sphenodon*), it may be possible that some lipids are also present extracellularly. The precise role of lipids on the waterproofing properties of alligator skin remains to be specifically analysed.

The present study supports earlier observations where it appeared that in crocodilians both the hinge region and the scutes are effective permeability barriers to water (Lillywhite & Maderson, 1982). This is different from lepidosaurian reptiles where the water barrier is mainly due to the mesos layer, and the β-layer has essentially a mechanical role (Landmann, 1979; Lillywhite & Maderson, 1982; Menon et al. 1996). During β-keratin differentiation in lepidosaurs lipid droplets are less frequently observed than in turtles and alligators, suggesting that their syncytial β-layer has less lipidogenic capability.

Pigmentation

Alligator skin is mostly pigmented by epidermal melanocytes from ES23 to ES25. Therefore, it is the continuous deposition of melanosomes into maturing β-keratinocytes (Szabo et al. 1973) that is predominantly responsible for the prehatching pattern. Dermal melanophores are involved in the young and adult skin pattern (Spearman, 1966; Spearman & Riley, 1969), although further studies on late embryos and young crocodilians are needed to confirm this notion. Epidermal melanocytes are distributed in small areas of the epidermis, along the margins and centre of scales, and are therefore responsible for the spot-like pigmentation of scales in young of *Crocodilus niloticus* (Spearman & Riley, 1969).

At ES25, epidermal melanocytes are more numerous than in previous stages and the dermis has become more pigmented, at least in some skin areas. Although not specifically studied, no cytological differences were observed between epidermal and dermal melanophores, suggesting that they are the same cells within the 2 tissues. Little cytological information is available for other reptiles (Lange, 1931; Cooper & Greenberg, 1992). In general, epidermal melanocytes seem to play the major role in the pigmentation, or morphological colour change, of turtle shell and skin of crocodilians (Cooper & Greenberg, 1992), whereas the morphological colour change in lepidosaurians results from movement of melanosomes from epidermal melanocytes within the epidermis (Szabo et al. 1973). In many lizards and snakes, dermal chromatophores are important for physiological colour changes, a process that is not present in turtles and crocodilians. Details on the modality of adult pigmentation pattern in crocodilians, and on the specific contribution of dermal melanosomes versus epidermal melanocytes remains to be investigated.

CONCLUSION

Our study provides the first detailed description of epidermal differentiation during the embryonic development of a crocodilian. In a series of studies, we have shown that the progressive transformation of an embryonic epidermis composed of α-keratin that contacts the amniotic fluid, is replaced by an adult epidermis of β-keratin in all reptilian lineages, including crocodilians (Fig. 35) (Dhouailly & Maderson, 1984; Alibardi, 1998*a*, *b*, 1999; Alibardi & Thompson, 1999*a*, *b*, *c*). Nevertheless, development of crocodilian skin shares some features of the β-keratin layers with birds, rather than with other reptiles, presumably reflecting the close phylogenetic relationship between crocodiles and birds (Matulionis, 1970; Kemp et al. 1974; Sawyer et al. 1974; Bowers & Brumbaugh, 1978). Thus, although the final structure of the skin of crocodiles and other reptiles share many features associated with the need for a tough skin in a terrestrial environment, the embryonic development of these features varies among lineages.

ACKNOWLEDGEMENTS

The visit to Sydney by LA was supported by the University of Bologna and by a Borsa Ghigi Award from the Accademia delle Scienze in Bologna. Mr Robert Porter and the Staff of the Australian Reptile Park in Gosford kindly supplied the eggs. Ms Kylie Russell helped with egg incubation in the laboratory; Ms Maria Petagine (Scuola di Disegno Anatomico, Bologna, Italy) drew Fig. 35; Mrs Luciana Dipietrangelo helped with photography. Some laboratory support was provided by an Australian Research Council Grant to MBT and all procedures conformed to the Australian NH&MRC code of practice for use of animals in research.

REFERENCES

ALEXANDER NJ (1970) Comparison of α and β keratin in reptiles. *Zeitschrift für Zellforschung* **110**, 153–165.

ALEXANDER NJ, PARAKKAL PF (1969) Formation of α- and β-type keratin in lizard epidermis during the molting cycle. *Zeitfrischt für Zellforschung* **101**, 72–87.

ALIBARDI L (1998*a*) Differentiation of the epidermis during scale formation in embryos of lizard. *Journal of Anatomy* **1926**, 173–186.

ALIBARDI L (1998*b*) Glycogen distribution in relation to epidermal cell differentiation during embryonic scale morphogenesis in the lizard *Anolis lineatopus*. *Acta Zoologica* **79**, 91–100.

ALIBARDI L (1998*c*) Presence of acid phosphatase in the epidermis of the regenerating tail of the lizard (*Podarcis muralis*) and its possible role in the process of shedding and keratinization. *Journal of Zoology* **246**, 379–390.

ALIBARDI L (1999) Keratohyalin-like granules in embryonic and regenerating epidermis of lizards and *Sphenodon punctatus* (Reptilia, Lepidosauria). *Amphibia-Reptilia* **20**, 11–23.

ALIBARDI L (2000) Keratinization and lipogenesis in the embryonic epidermis of the zebrafinch, *Taeniopygia guttata castanotis* (Aves, Passeriformlis, Ploecidae). *Journal of Morphology*, in press.

ALIBARDI L, THOMPSON MB (1999*a*) Epidermal differentiation in the developing scales of embryos of the Australian scincid lizard *Lampropholis guichenoti*. *Journal of Morphology* **241**, 139–152.

ALIBARDI L, THOMPSON MB (1999*b*) Epidermal differentiation during carapace and plastron formation in the embryonic turtle *Emydura macquarii*. *Journal of Anatomy* **194**, 531–545.

ALIBARDI L, THOMPSON MB (1999*c*) Morphogenesis of shell and scutes in the turtle *Emydura macquarii*. *Australian Journal of Zoology* **47**, 245–260.

ALLEN TD, POTTEN CS (1975) Desmosomal form, fate and function in mammalian epidermis. *Journal of Ultrastructure Research* **51**, 94–105.

BADEN HP, MADERSON PFA (1970) Morphological and biophysical identification of fibrous proteins in the amniote epidermis. *Journal of Experimental Zoology* **174**, 225–232.

BADEN HP, SVIOKLA S, ROTH I (1974) The structural protein of reptilian scales. *Journal of Experimental Zoology* **187**, 287–294.

BONNEVILLE M (1968) Observations on epidermal differentiation in the fetal rat. *American Journal of Anatomy* **123**, 147–164.

BOWERS RR, BRUMBAUGH JA (1978) An ultrastructural study of the regenerating breast feather of the fowl. *Journal of Morphology* **158**, 275–290.

BRAZAITIS P (1987) The identification of crocodilian skins and products. In *Wildlife Management: Crocodiles and Alligators* (ed. Webb G, Manolis S, Whitehead PJ), pp. 373–386. Chipping Norton: Surrey Beatty & Conservation Commission of the Northern Territory.

BRIGGAMAN RA, WHEELER CE (1975) The epidermal-dermal junction. *Journal of Investigative Dermatology* **65**, 71–84.

BUDZ PE, LARSEN LO (1975) Structure of the toad epidermis during the moulting cycle. *Cell & Tissue Research* **159**, 459–483.

CARVER WE, SAWYER RH (1987) Development and keratinization of the epidermis in the common lizard, *Anolis carolinensis*. *Journal of Experimental Zoology* **243**, 435–443.

CARVER WE, SAWYER RH (1988) Avian scale development: XI. Immunoelectron microscopic localization of α and β keratins in scutate scale. *Journal of Morphology* **195**, 31–43.

CARVER WE, SAWYER RH (1989) Immunocytochemical localization and biochemical analysis of α and β keratins in the avian lingual epithelium. *American Journal of Anatomy* **184**, 66–75.

COOPER WE, GREENBERG N (1992) Reptilian coloration and behavior. In *Biology of the Reptilia* (ed. Gans C, Billett F, Maderson PFA), vol. 18, Physiology E, pp. 298–423. Chicago-London: Chicago University Press.

DALE BA, HOLBROOK KA (1987) Developmental expression of human epidermal keratins and filaggrin. In *Cell and Molecular Biology of Keratins* (ed. Sawyer RH). *Current Topics in Developmental Biology*, vol. 22, pp. 127–151. New York: Academic Press.

DALE BA, HOLBROOK KA, KIMBALL JR, HOFF M, SUN TT (1985) Expression of epidermal keratins and filaggrin during human fetal skin development. *Journal of Cell Biology* **101**, 1257–1269.

DHOUAILLY D, MADERSON PFA (1984) Ultrastructural observations on the embryonic development of the integument of *Lacerta muralis* (Lacertilia, Reptilia). *Journal of Morphology* **179**, 203–228.

Du BRUL EF (1972) Fine structure of epidermal differentiation in the mouse. *Journal of Experimental Zoology* **181**, 145–158.

FERGUSON MWJ (1985) The reproductive biology and embryology of crocodilians. In *Biology of the Reptilia* (ed. Gans C, Billett F, Maderson PFA), vol. 14, *Development* B, pp. 329–491. New York: John Wiley & Sons.

FERGUSON MWJ (1987) Post-laying stages of embryonic development for crocodilians. In *Wildlife Management: Crocodiles and Alligators* (ed. Webb G, Manolis S, Whitehead PJ), pp. 427–444. Chipping Norton: Surrey Beatty & Conservation Commission of the Northern Territory.

FRAZER RDB, MCRAE TP, ROGERS GE (1972) *Keratins. Their Composition, Structure and Biosynthesis*. Springfield, IL, USA: Charles Thomas.

FREINKEL RK (1991) Carbohydrate metabolism of epidermis. In *Physiology, Biochemistry and Molecular Biology of the Skin*. 2nd edition (ed. Goldsmith LA), pp. 452–461. New York-Oxford: Oxford University Press.

FUKUYAMA K, EPSTEIN WL (1973) Heterogeneous ultrastructure of keratohyalin granules: a comparative study of adjacent skin and mucous membrane. *Journal of Investigative Dermatology* **61**, 94–100.

HAAKE AR, KONIG G, SAWYER RH (1984) Avian feather development: relationships between morphogenesis and keratinization. *Developmental Biology* **106**, 406–413.

HARDMAN MJ, SISI P, BANBURY DN, BYRNE C (1998) Pattern acquisition of skin barrier function during development. *Development* **125**, 1541–1552.

HARDY MH, SWEENY PR, BELLOWS CG (1978) The effects of vitamin A on the epidermis of the fetal mouse in organ culture. An ultrastructural study. *Journal of Ultrastructure Research* **64**, 246–260.

HASHIMOTO K (1971) Ultrastructure of the human toenail. II. Keratinization and formation of the marginal band. *Journal of Ultrastructure Research* **36**, 391–410.

IRISH FJ, WILLIAMS EE, SEILING E (1988) Scanning electron microscopy of changes in epidermal structure occurring during the shedding cycle in squamate reptiles. *Journal of Morphology* **197**, 105–126.

KEMP DJ, DYER PY, ROGERS GE (1974) Keratin synthesis during development of the embryonic chick feather. *Journal of Cell Biology* **62**, 114–131.

LANDMANN L (1979) Keratin formation and barrier mechanisms in the epidermis of *Natrix natrix* (Reptilia: Serpentes): an ultrastructural study. *Journal of Morphology* **162**, 93–126.

LANDMANN L (1980) Lamellar granules in mammalian, avian, and reptilian epidermis. *Journal of Ultrastructure Research* **72**, 245–263.

LANDMANN L (1986) The skin of Reptiles: epidermis and dermis. In *Biology of the Integument* (ed. Bereiter-Hahn J, Matoltsy AG, Sylvia-Richards K), vol. 2, *Vertebrates*, pp. 150–187. Berlin: Springer.

LANGE B (1931) Integument der sauropsiden. In *Handbuch der vergleichendend Anatomie der Wirbeltiere* (ed. Bolk L, Goppert E, Kallius E, Lubosch W), vol. 1, pp. 375–448. Berlin: Urban & Schwarzenberg.

LILLYWHITE HB, MADERSON PFA (1982) Skin structure and permeability. In *Biology of the Reptilia* (ed. Gans C, Pough FH), vol. 12, *Physiological Ecology*, pp. 397–442. New York and London: Academic Press.

LYNE AG, HOLLIS PFA (1972) The structure and development of the epidermis in the sheep. *Journal of Ultrastructure Research* **38**, 444–458.

MADERSON PFA (1985) Some developmental problems of the reptilian integument. In *Biology of the Reptilia* (ed. Gans C,

Billett F, Maderson PFA), vol. 256 14, *Development* B, pp. 525–598. New York: John Wiley & Sons.

MADERSON PFA, ALIBARDI L (2000) The development of the sauropsid integument: review and comments. *American Zoologist* **40**, in press.

MADERSON PFA, FLAXMAN BA, ROTH SI, SZABO G (1972) Ultrastructural contribution to the identification of cell types in the lizard epidermal generation. *Journal of Morphology* **136**, 191–210.

MADERSON PFA, RABINOWITZ T, TANDLER B, ALIBARDI L (1998) Ultrastructural contributions to an understanding of the cellular mechanisms involved in lizard skin shedding with comments on the function and evolution of a unique lepidosaurian phenomenon. *Journal of Morphology* **236**, 1–24.

MARSHALL RC, ORWIN DFG, GILLESPIE JM (1991) Structure and biochemistry of mammalian hard keratin. *Electron Microscopic Review* **4**, 47–83.

MATOLTSY AG (1987) Cell and molecular biology of keratins. Concluding remarks and future directions. In *Topics in Developmental Biology* (ed. Moscona AA, Monroy A), vol. 22, pp. 255–264. New York, London: Academic Press.

MATOLTSY AG, BEREITER-HAHN J (1986) Biology of the integument. Introduction. In *Biology of the Integument* (ed. Bereither-Hahn, Matoltsy JAG, Sylvia-Richards K), vol. 2, *Vertebrates*, pp. 1–7. Berlin: Springer.

MATOLTSY AG, HUSZAR T (1972) Keratinization of the reptilian epidermis: and ultrastructural study on the reptilian skin. *Journal of Ultrastructure Research*, **38**, 87–101.

MATULIONIS DH (1970) Morphology of the developing down feathers of chick embryos. *Zeitfrischt für Anatomie und Entwicklungs-Geschichte* **132**, 107–157.

MAYER W, BAUMGARTNER G (1998) Embryonal feather growth in the chicken. *Journal of Anatomy* **193**, 611–616.

MAZZI V (1977) *Manuale di Tecniche Istologiche e Istochimiche*. Padova: Piccin Editore.

MENON GK, BROWN BE, ELIAS PM (1986) Avian epidermal differentiation: role of lipids in permeability barrier function. *Tissues and Cell* **18**, 71–82.

MENON GK, GHADIALLY R, WILLIAMS ML, ELIAS PM (1992) Lamellar bodies as delivery systems of hydrolytic enzymes: implications for normal and abnormal desquamation. *British Journal of Dermatology* **126**, 337–345.

MENON GK, MADERSON PFA, DREWES RC, BAPTISTA LF, PRICE LF, ELIAS PM (1996) Ultrastructural organization of avian stratum corneum lipids as the basis for facultative cutaneous waterproofing. *Journal of Morphology* **227**, 1–13.

MOTTET NK, JENSEN HM (1968) The differentiation of chick embryonic skin. *Experimental Cell Research* **52**, 261–283.

PARAKKAL PF, ALEXANDER NJ (1972) *Keratinization. A Survey of Vertebrate Epithelia*. New York, London: Academic Press.

PARAKKAL PF, MATOLTSY GA (1968) An electron microscopic study of developing chick skin. *Journal of Ultrastructure Research* **23**, 403–416.

ROTH SI, JONES WA (1970) The ultrastructure of epidermal maturation in the skin of the boa constrictor (*Constrictor constrictor* 256). *Journal of Ultrastructural Research* **32**, 69–93.

SAWYER RH, ABBOTT UK, FRY GN (1974) Avian scale development. III. Ultrastructure of the keratinizing cells of the outer and inner epidermal surfaces of the scale ridge. *Journal of Experimental Zoology* **190**, 57–70.

SAWYER RH, KNAPP LW, O'UIN MW (1986) Epidermis, dermis and appendages. In *Biology of the Integument* (ed. Bereither-Hahn J, Matoltsy AG, Sylvia-Richards R), vol. 2, *Vertebrates*, pp. 194–237. Berlin: Springer.

SAWYER RH, GLENN T, FRENCH JO, MAYS B, SHAMES RB, BARNES GL Jr et al. (2000) The expression of beta-keratin in the epidermal appendages of reptiles and birds. *American Zoologist* **40 (**in press**).**

SHAMES RB, KNAPP LW, CARVER WE, SAWYER RH (1988) Identification, expression, and localization of keratin gene products during development of avian scutate scales. *Differentiation* **38**, 115–123.

SHAMES RB, KNAPP LW, CARVER WE, WASHINGTON LD, SAWYER RH (1989) Keratinization of the outer surface of the avian scutate scale: interrelationship of alpha and beta keratin filaments in a cornifying tissue. *Cell and Tissue Research* **257**, 85–92.

SHAMES RB, KNAPP LW, CARVER WE, WASHINGTON LD, SAWYER RH (1991) Region-specific expression of scutate scale type beta keratins in the developing chick beak. *Journal of Experimental Zoology* **260**, 258–266.

SPEARMAN RIC (1966) The keratinization of epidermal scales, feathers and hairs. *Biological Reviews* **41**, 59–96.

SPEARMAN RIC, RILEY PA (1969) A comparison of the epidermis and pigment cells of the crocodile with those in two lizard species. *Zoological Journal of the Linnean Society* **48**, 453–466.

SPEARMAN RIC, HARDY JA (1985) Integument. In *Form and Function in Birds* (ed. King AS & McLelland J), vol. 3, pp. 1–56. Academic Press: London, Tokyo.

SZABO G, MADERSON PFA, ROTH SI, KOSTICK RM (1973) Melanocyte activity in the epidermis of the boa constrictor (Constrictor constrictor) during the sloughing cycle. *Anatomical Record* **176**, 377–388.

WEISS LW, ZELICKSON AS (1975*a*) Embryology of the epidermis: ultrastructural aspects. I) Formation and early differentiation of the mouse with mammalian comparison. *Acta Dermatologica* (*Stockolm*) **55**, 161–168.

WEISS LW, ZELICKSON AS (1975*b*) Embryology of the epidermis: ultrastructural aspects. II) Period of differentiation in the mouse with mammalian comparison. *Acta Dermatovener* (*Stockolm*) **55**, 321–329.

WEISS LW, ZELICKSON AS (1975*c*) Embryology of the epidermis: ultrastructural aspects. III) Maturation and primary appearence of dendritic cells in the mouse with mammalian comparison. *Acta Dermatovenerologica* (*Stockolm*) **55**, 431–442.

WYLD JA, BRUSH AH (1979) The molecular heterogeneity and diversity of reptilian keratins. *Journal of Molecular Evolution* **12**, 331–347.

WYLD JA, BRUSH AH (1983) Keratin diversity in the reptilian epidermis. *Journal of Experimental Zoology* **225**, 387–396.